Electronic Supplementary Information

Noncovalent Molecular Interactions, Charge Transport and Photovoltaic Performance of Asymmetric M-Series Acceptors with Dichlorinated End Groups

Ruochuan Liao,[ac] Xiaoling Ma,[d] Changquan Tang,[a] Yuanzheng Liu,[a] Wenyu Zheng,[e] Yunlong Ma,[a] Qisheng Tu,[a] Wenyuan Lin,[a] Yuanping Yi,[e] and Qingdong Zheng[ab]*

[a] State Key Laboratory of Structural Chemistry, Fujian Institute of Research on the Structure of Matter, Chinese Academy of Sciences, 155 Yangqiao Road West, Fuzhou, Fujian 350002, China

[b] State Key Laboratory of Coordination Chemistry, College of Engineering and Applied Sciences, Nanjing University, Nanjing 210023, China

[c] University of Chinese Academy of Sciences, Beijing 100049, China

[d] School of Science, Beijing Jiaotong University, Beijing 100044, China

[e] Beijing National Laboratory for Molecular Sciences, CAS Key Laboratory of Organic Solids, Institute of Chemistry, Chinese Academy of Sciences, Beijing 100190, China

** Corresponding author: E-mail: qingdongzheng@fjirsm.ac.cn*

Table of Contents

1. Materials and instruments

PM6 was purchased from Solarmer Materials Inc. Other solvents and reagents were purchased from Bidepharm Ltd., Adamas-beta Ltd., or Energy-Chemical Ltd., and used directly without further purification unless stated otherwise. High-resolution mass spectroscopy (HRMS) measurements were performed on a Thermo Scientific QExactive mass spectrometer. ^{1}H and ^{13}C NMR spectra were acquired on a Bruker AVANCE III HD nuclear magnetic resonance spectrometer. Elemental analyses were obtained from a Vario EL-Cube elemental analyzer. UV-vis absorption spectra were carried out by a Lambda950 UV-vis spectrophotometer. Photoluminescence spectra were recorded from an Edinburgh Instrument FLS 920. All the films for absorption and photoluminescence experiments were annealed at 80 ^{o}C for 5 min. The thickness of film was determined by a Bruker Dektak XT surface profilometer. Atomic force microscopy (AFM) images were obtained from a Bruker Nanoscale V station at a tapping mode. Cyclic voltammetry (CV) experiments were conducted on a CHI 604E electrochemical workstation at a scan rate of 100 mV s^{-1} with a three-electrode cell in a nitrogen bubbled 0.1 M Bu_4NPF_6 solution in acetonitrile at room temperature. Platinum wire, $Ag/AgNO_3$ (0.1 M $AgNO_3$ in acetonitrile) and platinum plate were used as the counter electrode, reference electrode and working electrode, respectively. The $Ag/AgNO_3$ reference electrode was calibrated using a ferrocene/ferrocenium redox couple as an external standard, whose oxidation potential is set at -4.80 eV with respect to zero vacuum level. Under this condition, the onset oxidation potential of ferrocene was -0.02 V *versus* Ag/Ag^{+}. The neat films of acceptors on the Pt plate electrode were obtained by dipping the electrode into corresponding chloroform solutions. The HOMO and LUMO energy level were calculated by using the equations of $E_{HOMO} = -(\varphi_{ox} + 4.82)$ (eV) and $E_{LUMO} = -(\varphi_{red} + 4.82)$ (eV), respectively.

2. Synthesis

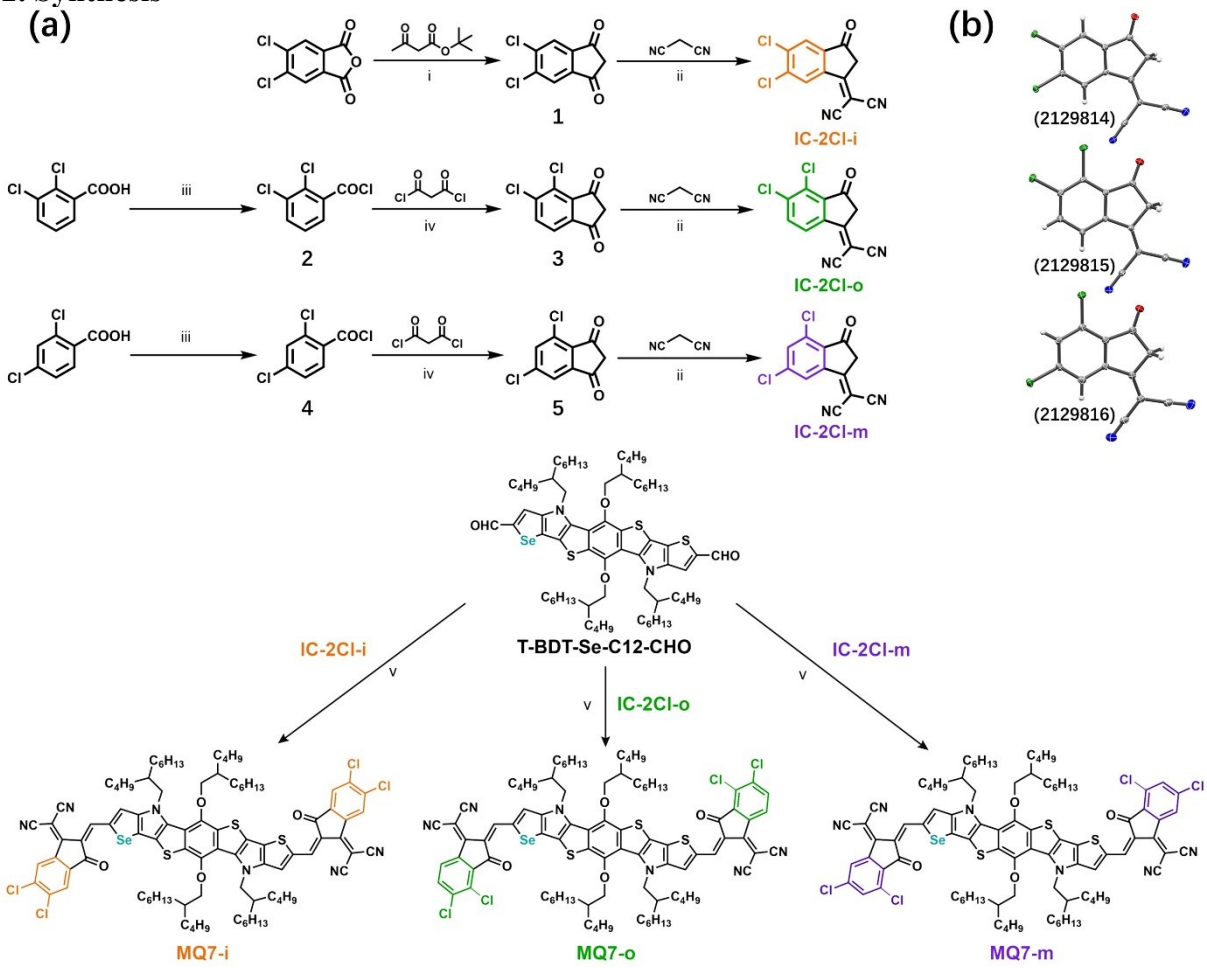

Scheme S1. (a) Synthetic route to **MQ7-i**, **MQ7-o** and **MQ7-m**. Reagents and conditions: i) Et_3N, Ac_2O, 65 °C, overnight; ii) NaOAc, EtOH, 55°C, iii) $SOCl_2$, DMF, $CHCl_3$, reflux, 3 h; iv) DCE/DCM, $AlCl_3$, reflux, overnight; v) pyridine, $CHCl_3$, 55°C. (b) Single crystal structures and relative CCDC deposition numbers of terminal groups.

Compound 1: Under the protection of N_2, a 100 mL oven dried round-bottom flask was charged in turn with 5,6-dichloroisobenzofuran-1,3-dione (2.00 g, 9.22 mmol, 1.0 equiv.), acetic anhydride (20 mL), triethylamine (8 mL) and *tert*-butyl acetoacetate (2.18 g, 13.8 mmol, 1.5 equiv.). The reaction was stirred at 65 °C overnight. After cooling to room temperature, the reaction mixture was poured into HCl (4M, aq.) and heated to 80 °C for 1 h. The mixture was filtered by vacuum filtration through a Buchner funnel. The solid was washed with H_2O and dried under vacuum to yield the crude product as a brown powder (1.78 g, 89%) that was directly used without further purification.

Compound IC-2Cl-i: Under the protection of N_2, a 50 mL oven dried round-bottom flask was charged in turn with **1** (1.00 g, 4.65 mmol, 1.0 equiv.), sodium acetate (0.572 g, 6.98 mmol, 1.5 equiv.), anhydrous ethanol (10 mL) and malononitrile (0.614 g, 9.30 mmol, 2.0 equiv.). The

mixture was stirred at room temperature and monitored by TLC. After several hours, the mixture was poured into 80 mL water, and acidified to pH=1-2 by using HCl. The solid was filtered and purified by column chromatography (SiO_2: CH_2Cl_2: petroleum ether 50:50 to 100:0), and then recrystallized with hexane, to obtain **IC-2Cl-i** as a light yellow solid (0.681g, 56%).

Compound 2: In a 100 mL oven dried round-bottom flask, thionyl chloride (9.94 g, 83.6 mmol, 4.0 equiv.) was added to a solution of 2,3-dichlorobenzoic acid (4.00 g, 20.9 mmol, 1.0 equiv.) in 40 mL of dry chloroform under the protection of N_2. 0.4 mL of dry DMF was added dropwise into the reaction. The mixture was heated to reflux for 3 h. After cooling to room temperature, the excess thionyl chloride was removed under the reduced pressure. The product was directly used without further purification.

Compound 3[1]: After purged with N_2 for 30 minutes, the solution of **2** (20.9 mmol) in 20 mL of dry 1,2-dichloroethane was transferred into $AlCl_3$ (12.5 g, 94.0 mmol, 4.5 equiv.) in dry dichloromethane (40 mL) solution. Under the protection of N_2, malonyl dichloride (13.2 g, 94.0 mmol, 4.5 equiv.) was added dropwise into the mixture. The reaction was heated to reflux overnight. After cooling to 10°C, the mixture was carefully poured into 100 mL of ice-water and acidified with 80 mL of HCl (6M, aq.). The mixture was poured into a separatory funnel, and the aqueous layer was extracted with dichloromethane (3 x 100 mL). The combined organics were washed with brine, dried over $MgSO_4$, filtered, and concentrated under reduced pressure. The crude product was then purified by column chromatography (SiO_2, CH_2Cl_2: petroleum ether=50:50 to 100:0) to afford a pale powder (1.14 g, 26%). ^{1}H NMR (400 MHz, $CDCl_3$): δ = 7.91 (d, 1H, J=8.0 Hz), 7.84 (d, 1H, J=8.0 Hz), 3.32 (s, 2H). ^{13}C NMR (101 MHz, $CDCl_3$): δ = 194.84, 193.33, 143.07, 142.13, 139.81, 136.90, 130.18, 121.82, 45.28. FT-MS m/z: calcd for $C_9H_4Cl_2O_2$ $[M-H]^-$: 213.0; Found: 213.0.

Compound IC-2Cl-o: Under the protection of N_2, a 50 mL oven dried round-bottom flask was in turn charged with **3** (1.00 g, 4.65 mmol, 1.0 equiv.), sodium acetate (0.572 g, 6.98 mmol, 1.5 equiv.), anhydrous ethanol (20 mL) and malononitrile (0.614 g, 9.30 mmol, 2.0 equiv.). The mixture was stirred at room temperature and monitored by TLC. After several hours, the mixture was poured into 80 mL of water, and acidified to pH=1-2 by using HCl. The solid was filtered and purified by column chromatography (SiO_2: CH_2Cl_2: petroleum ether 50:50 to 100:0), and then recrystallized with hexane, to obtain **IC-2Cl-o** as a light-yellow solid (0.856 g, 70%). ^{1}H NMR (400 MHz, $CDCl_3$): δ = 8.53 (d, 1H, J=8.4 Hz), 7.94 (d, 1H, J=8.4 Hz), 3.81

(s, 2H). ^{13}C NMR (101 MHz, $CDCl_3$): δ = 190.86, 163.19, 142.41, 142.10, 137.00, 136.91, 132.00, 124.34, 111.89, 111.67, 80.14, 43.92. FT-MS m/z: calcd for $C_{12}H_4Cl_2N_2O$ $[M-H]^-$: 261.0; Found: 261.0.

Compound 4: In a 100 mL oven dried round-bottom flask, thionyl chloride (9.94 g, 83.6 mmol, 4.0 equiv.) was added to a solution of 2,4-dichlorobenzoic acid (4.00 g, 20.9 mmol, 1.0 equiv.) in 40 mL of dry chloroform under the protection of N_2. Dry DMF (0.4 mL) was added dropwise into the reaction. The mixture was heated to reflux for 3 h. After cooling to room temperature, the excess thionyl chloride was removed under the reduced pressure. The product was directly used without further purification.

Compound 5: After purged with N_2 for 30 minutes, the solution of **4** (20.9 mmol) in 20 mL dry 1,2-dichloroethane was transferred into $AlCl_3$ (12.5 g, 94.0 mmol, 4.5 equiv.) in dry dichloromethane (40 mL) solution. Under the protection of N_2, malonyl dichloride (13.2 g, 94.0 mmol, 4.5 equiv.) was added dropwise into the mixture. The reaction was heated to reflux overnight. After cooling to 10°C, the mixture was carefully poured into 100 mL of ice-water and acidified with 80 mL of HCl (6M, aq.). The mixture was poured into a separatory funnel, and the aqueous layer was extracted with dichloromethane (3 x 100 mL). The combined organics were washed with brine, dried over $MgSO_4$, filtered, and concentrated under reduced pressure. The crude product was then purified by column chromatography (SiO_2, CH_2Cl_2: petroleum ether=50:50 to 100:0) to afford a pale powder (0.984 g, 22%). ^{1}H NMR (400 MHz, $CDCl_3$): δ =7.85 (d, 1H, J=1.6 Hz), 7.76 (d, 1H, J=1.6 Hz), 3.32 (s, 2H). ^{13}C NMR (101 MHz, $CDCl_3$): δ =194.75, 193.06, 145.73, 142.57, 136.91, 136.84, 132.79, 121.93, 45.42. FT-MS m/z: calcd for $C_9H_4Cl_2O_2$ $[M-H]^-$: 213.0; Found: 213.0.

Compound IC-2Cl-m: Under the protection of N_2, a 50 mL oven dried round-bottom flask was in turn charged with **12** (0.800 g, 3.72 mmol, 1.0 equiv.), sodium acetate (0.845 g, 5.58 mmol, 1.5 equiv.), anhydrous ethanol (10 mL) and malononitrile (0.491 g, 7.44 mmol, 2.0 equiv.). The mixture was stirred at room temperature and monitored by TLC. After several hours, the mixture was poured into 40 mL of water, and acidified to pH=1-2 by using HCl. The solid was filtered and purified by column chromatography (SiO_2, CH_2Cl_2: petroleum ether=50:50 to 100:0), and then recrystallized with hexanes, to obtain **IC-2Cl-m** as a colorless crystal (0.726 g, 74%).^{1}H NMR (400 MHz, $CDCl_3$): δ = 8.54 (d, 1H, J=1.6 Hz), 7.77 (d, 1H, J=1.6 Hz), 3.79 (s, 2H). ^{13}C NMR (101 MHz, $CDCl_3$): δ = 190.60, 163.12, 144.96, 142.95, 136.80, 134.25,

134.06, 124.36, 111.52, 111.44, 81.21, 43.89. FT-MS m/z: calcd for $C_{12}H_4Cl_2N_2O$ $[M-H]^-$: 261.0; Found: 261.0.

MQ7-i: Under the protection of N_2, a 50 mL oven dried two-neck round-bottom flask was in turn charged with **T-BDT-Se-C12-CHO** (120 mg, 0.101 mmol, 1.0 equiv.), chloroform (20 mL) and pyridine (0.1 mL). After the solution was bubbled with N_2 for 20 min, **IC-2Cl-i** (133 mg, 0.455 mmol, 5.0 equiv.) was added. Then the solution was stirred at 50℃ for 8 h. After removing the solvent, the mixture was purified by column chromatography (SiO_2, CH_2Cl_2: petroleum ether=60:40 to 50:50) to obtain **MQ7-i** as a dark blue solid (151 mg, 89%). ^{1}H NMR (400 MHz, $CDCl_3$): δ = 9.11 (s, 1H), 8.98 (s, 1H), 8.76 (s, 1H), 8.74 (s, 1H), 8.01 (s, 1H), 7.95-7.94 (m, 2H), 7.91 (s, 1H), 4.76 (t, J = 7.8 Hz, 4H), 4.04-4.02 (m, 4H), 2.16–2.08 (m, 2H), 2.03–1.93 (m, 2H), 1.71–1.63 (m, 4H), 1.57–1.49 (m, 4H), 1.42–1.32 (m, 24H), 1.24–1.17 (m, 4H), 1.16–1.02 (m, 28H), 0.97 (t, J = 6.8 Hz, 6H), 0.92 (t, J = 6.8 Hz, 6H), 0.76 (t, J = 6.8 Hz, 6H), 0.70 (t, J = 6.8 Hz, 6H). ^{13}C NMR (101 MHz, $CDCl_3$): δ = 186.62, 185.93, 158.44, 158.19, 149.51, 148.16, 145.65, 145.15, 145.03, 145.01, 142.18, 139.37, 139.32, 139.26, 139.08, 138.93, 138.67, 138.62, 138.26, 137.55, 137.25, 137.11, 136.07, 135.97, 134.21, 133.03, 131.42, 127.18, 126.76, 125.03, 121.69, 120.59, 120.30, 120.01, 119.55, 117.34, 114.90, 114.81, 114.69, 114.64, 79.59, 79.53, 68.30, 67.97, 52.94, 39.27, 39.22, 39.13, 38.95, 31.93, 31.63, 31.17, 31.13, 30.81, 30.79, 30.62, 30.35, 29.82, 29.51, 29.17, 28.00, 27.00, 26.95, 25.78, 23.17, 22.89, 22.74, 22.57, 14.19, 14.06, 13.84. MALDI-HRMS *m/z*: calcd for $C_{92}H_{108}Cl_4N_6O_4S_3Se$ $[M+H]^+$: 1677.5547; Found: 1677.5568. Elemental analysis (%) calcd for $C_{92}H_{108}Cl_4N_6O_4S_3Se$: C 65.82, H 6.48, N 5.01; Found: C 65.53, H 6.39, N 4.80.

MQ7-o: The acceptor **MQ7-o** was synthesized according to the same preparative procedure as that for **MQ7-i**. Quantities: **T-BDT-Se-C12-CHO** (90 mg, 0.076 mmol, 1.0 equiv.), pyridine (0.1 mL), **IC-2Cl-o** (100 mg, 0.38 mmol, 5.0 equiv.) and chloroform (18 mL). **MQ7-o** was obtained as a dark blue solid (102 mg, 80%). ^{1}H NMR (400 MHz, $CDCl_3$): δ = 9.14 (s, 1H), 9.03 (s, 1H), 8.58-8.55 (m, 2H), 8.01 (s, 1H), 7.84 (s, 1H), 7.84-7.76 (m, 2H), 4.76 (t, J = 8.0 Hz, 4H), 4.04-4.01 (m, 4H), 2.16–2.08 (m, 2H), 2.03–1.93 (m, 2H), 1.71–1.63 (m, 4H), 1.57–1.49 (m, 4H), 1.42–1.32 (m, 24H), 1.24–1.17 (m, 4H), 1.16–1.02 (m, 28H), 0.97 (t, J = 6.8 Hz, 6H), 0.92 (t, J = 6.8 Hz, 6H), 0.76 (t, J = 6.8 Hz, 6H), 0.70 (t, J = 6.8 Hz, 6H). ^{13}C NMR (101 MHz, $CDCl_3$): δ = 185.69, 185.07, 157.70, 157.53, 149.59, 148.12, 145.67, 145.14, 145.00, 142.18, 140.19, 140.11, 140.00, 139.88, 139.48, 138.14, 137.50, 137.24, 137.14, 135.26, 135.22, 134.45, 133.37, 133.18, 131.36, 130.93, 130.83, 127.33, 123.64, 123.61, 121.66, 120.54, 120.30, 120.03, 119.60, 117.33, 115.10, 115.02, 114.97, 79.61, 79.55, 67.73, 67.39,

52.92, 39.29, 39.23, 39.11, 38.93, 31.92, 31.62, 31.24, 31.18, 30.87, 30.83, 30.62, 30.34, 29.82, 29.50, 29.21, 29.15, 28.00, 27.06, 26.99, 25.77, 23.16, 22.88, 22.74, 22.56, 14.18, 14.06, 13.83. MALDI-HRMS m/z: calcd for $C_{92}H_{108}Cl_4N_6O_4S_3Se$ $[M+H]^+$: 1677.5547; Found: 1677.5554. Elemental analysis (%) calcd for $C_{92}H_{108}Cl_4N_6O_4S_3Se$: C 65.82, H 6.48, N 5.01; Found: C 65.83, H 6.50, N 4.86.

MQ7-m: The acceptor **MQ7-m** was synthesized according to the same preparative procedure as that for **MQ7-i**. Quantities: **T-BDT-Se-C12-CHO** (90 mg, 0.076 mmol, 1.0 equiv.), pyridine (0.1 mL), **IC-2Cl-m** (100 mg, 0.38 mmol, 5.0 equiv.) and chloroform (18 mL). **MQ7-m** was obtained as a dark blue solid (119 mg, 94%). ^{1}H NMR (400 MHz, $CDCl_3$): δ = 9.14 (s, 1H), 9.02 (s, 1H), 8.61-8.59 (m, 2H), 8.00 (s, 1H), 7.84 (s, 1H), 7.64–7.62 (m, 2H), 4.75 (t, J = 7.8 Hz, 4H), 4.02-4.00 (m, 4H), 2.15–2.07 (m, 2H), 2.02–1.94 (m, 2H), 1.71–1.60 (m, 4H), 1.57–1.49 (m, 4H), 1.42–1.32 (m, 24H), 1.24–1.17 (m, 4H), 1.16–1.02 (m, 28H), 0.97 (t, J = 6.4 Hz, 6H), 0.92 (t, J = 6.4 Hz, 6H), 0.76 (t, J = 6.8 Hz, 6H), 0.70 (t, J = 6.8 Hz, 6H). ^{13}C NMR (101 MHz, $CDCl_3$): δ = 185.62, 184.97, 157.38, 157.18, 149.66, 148.18, 145.80, 145.18, 145.14, 145.04, 142.95, 142.89, 142.16, 141.08, 141.04, 139.45, 138.23, 137.59, 137.29, 137.19, 135.14, 135.04, 134.72, 133.57, 133.12, 133.00, 131.43, 130.03, 129.99, 127.39, 123.70, 121.75, 120.57, 120.32, 120.05, 119.61, 117.41, 114.99, 114.89, 114.72, 114.65, 79.63, 79.57, 68.24, 67.85, 52.92, 39.29, 39.24, 39.12, 38.94, 31.92, 31.62, 31.23, 31.17, 30.85, 30.82, 30.61, 30.34, 29.83, 29.81, 29.50, 29.21, 29.15, 28.00, 27.06, 26.99, 25.77, 23.16, 22.88, 22.74, 22.56, 14.18, 14.06, 13.83. MALDI-HRMS m/z: calcd for $C_{92}H_{108}Cl_4N_6O_4S_3Se$ $[M+H]^+$: 1677.5547; Found: 1677.5547. Elemental analysis (%) calcd for $C_{92}H_{108}Cl_4N_6O_4S_3Se$: C 65.82, H 6.48, N 5.01; Found: C 66.05, H 6.55, N 4.84.

3. Computational details

The optimized conformations of the acceptors were obtained by the DFT method at the B3LYP-D3(BJ)/6-31G(d) level. To reduce the computational costs, the long branched alkyl chains were replaced by isobutyl groups for the HOMO and LUMO calculations. DFT calculation was carried out with the Gaussian 09 program package. For the electronic couplings calculation, all geometry optimizations were performed by using Gaussian 09 at the B3LYP/6-31G level.

4. OSC device fabrication and characterization

The OSC devices were fabricated with the configuration of ITO/PEDOT:PSS/active layer/PDIN/Ag. ITO-coated glass substrates were cleaned by ultrasonicating sequentially in detergent, deionized water, acetone, and isopropanol for 10 min each and then dried in an oven

at 80 °C for 12 h. Then, the ITO glass substrates were subjected to ultraviolet/ozone treatment at room temperature for 15 min. The filtered PEDOT:PSS solution (Baytron PVP AI 4083 from H. C. Starck) was spin-coated onto the cleaned ITO substrates at 3500 rpm, followed by baking at 140 °C for 15 min in air. Subsequently, the substrates were transferred into a N_2-filled glove box for spin-coating the active layer. The blend solutions for the active layer (total concentration of 16 mg mL^{-1}) with 0.5 % (vol. %) 1-chloronaphthalene (CN) as additive, were prepared at 50 °C in chloroform. The mixed solutions were spin-coated on the top of the PEDOT:PSS layer at 3500 rpm for 30 s followed by thermal annealing at 80 °C for 5 min to form the active layer with a thickness of ~150 nm. PDIN methanol solution (2.0 mg/mL) was then spin-coated on the active layer at 3000 rpm for 30 s to afford a buffer layer with a thickness of ca. 10 nm. Finally, 100 nm of Ag top electrode was deposited onto the PDIN buffer layer through shadow masks by thermal evaporation at a pressure of 1.0×10^{-4} Pa. The deposition rate and film thickness were monitored with a quartz crystal sensor. The active area of the devices was 4 mm^2. After an encapsulation by epoxy kits (general purpose, Sigma-Aldrich) in the glovebox, the devices were illuminated through the ITO side.

The current density-voltage (*J-V*) characteristics were measured using a Keithley 2400 Source-Measure Unit. An Oriel Sol3A simulator (Newport) was used as a light source. The light intensity was calibrated to 100 mW cm^{-2} by a NREL-certified silicon reference cell. More than 8 devices were measured to provide the average PCEs of PSCs. EQE data were taken by using the QE/IPCE measurement kit (QE-PV-SI) from Newport.

5. Hole- and electron-only device fabrication and characterization

Hole- and electron- mobilities were measured using the space charge limited current (SCLC) method. Hole-only devices were fabricated with an architecture of ITO/PEDOT:PSS/active layer/MoO_3/Ag, while electron-only devices were constructed with an architecture of ITO/ZnO/active layer/Ca/Al. The active layers were prepared using the same method as that used for the best-performance OSCs fabrication. Device areas were fixed at 4 mm^2. The current density (*J*) was measured by a Keithley 2440 source measurement unit. The SCLC hole/electron mobilities were calculated according to the following equation:

$$J = \frac{9}{8}\varepsilon_r\varepsilon_0\mu\frac{V^2}{L^3}$$

Where *J* is the current density (A m^{-2}), ε_0 is the free-space permittivity (8.85×10^{-12} F m^{-1}), ε_r is the relative dielectric constant of the active layer material (usually 2-4 for organic semiconductors, herein we used a relative dielectric constant of 3), μ is the mobility of hole or electron, *V* is the voltage drop across the SCLC device ($V = V_{appl}-V_{bi}$, where V_{appl} is the applied voltage to the device and V_{bi} is the built-in voltage due to the difference in the work function of two electrodes in the hole- and electron-only devices, the V_{bi} values are 0.5 and 0.7 V, respectively), and L is the thickness of the active layer. The thickness of the film was

determined by a Bruker Dektak XT surface profilometer. The hole- or electron-mobility can be calculated from the slope of the $J^{1/2}$-V curves.

6. X-ray crystallographic analysis

Single crystal growth: diffraction quality crystal of **MQ7-i** was successfully prepared by solvent diffusion growth method from the poor solvent methanol to the good solvent toluene. Diffraction quality crystal of **MQ7-m** was prepared by vapor diffusion growth method from the poor solvent ether to the good solvent toluene. Diffraction quality crystal of **MQ7-o** was prepared by solvent diffusion growth method from the poor solvent methanol to the good solvent dibromomethane.

Well diffracting crystals of **MQ7-i** and **MQ7-m** (black lustrous prisms with a golden gloss) were selected and recorded on a XtaLAB Synergy, Dualflex, HyPix diffractometer with Cu Kα radiation (λ = 1.54178 Å) at 100 K. The counterpart of **MQ7-o** were selected and recorded on a ROD, Synergy Custom system, HyPix diffractometer with Ga Kα radiation (λ = 1.3405 Å) at 100 K. Using Olex2, the structure was solved with the ShelXT structure solution program using Intrinsic Phasing method and refined with the XL refinement package using Least Squares minimization. Because of the weak diffraction intensity, the alkyl carbon atoms were highly disordered and some of them could not be located. Contributions to scattering due to disordered solvent molecules were removed using the SQUEEZE routine of PLATON; structures were then refined again using the data generated. Crystal data and details of data collection and refinement of **MQ7-i**, **MQ7-o** and **MQ7-m** were summarized in **Table S2**. Crystal data and details of data collection and refinement of **IC-2Cl-i**, **IC-2Cl-o** and **IC-2Cl-m** were summarized in **Table S1**.

7. GIWAXS characterization

All samples for GIWAXS measurement were prepared on the PEDOT:PSS-coated Si substrates. The 2D GIWAXS patterns were acquired using a XEUSS SAXS/WAXS system at the National Center for Nanoscience and Technology (NCNST, Beijing). The wavelength of the X-ray beam is 1.54 Å, and the incident angle was set as 0.2˚. Scattered X-rays were detected by using a Dectris Pilatus 300 K photon counting detector. The coherence length was estimated by the Scherrer equation: CL= 2πk/FWHM, where FWHM is the full width at half-maximum of the peak and k is a shape factor (0.9 was used here).

8. Supplementary tables

Table S1. Crystal structure data and structural refinement for **IC-2Cl-i**, **IC-2Cl-o** and **IC-2Cl-m**.

Compound	IC-2Cl-i	IC-2Cl-o	IC-2Cl-m
CCDC Number	2129814	2129815	2129816
Empirical formula	$C_{12}H_4Cl_2N_2O$	$C_{12}H_4Cl_2N_2O$	$C_{24}H_8Cl_4N_4O_2$
Formula weight	262.06	263.07	526.14
Temperature/K	100.01(16)	298	100.01(10)
Crystal system	monoclinic	monoclinic	monoclinic
Space group	$P2_1/n$	$P2_1/n$	$P2_1/n$
a/Å	6.23030(10)	9.7923(3)	6.63540(10)
b/Å	10.92950(10)	6.8884(2)	9.6114(2)
c/Å	15.8006(2)	16.7454(5)	35.5446(5)
α/°	90	90	90
β/°	93.4430(10)	94.518(3)	91.5550(10)
γ/°	90	90	90
Volume/Å^3	1073.98(2)	1126.02(6)	2266.04(7)
Z	4	4	4
ρ_{calc}g/cm^3	1.621	1.552	1.542
μ/mm^{-1}	5.293	3.348	5.017
F(000)	524.0	528.0	1056.0
Crystal size/mm^3	0.03 × 0.03 × 0.2	0.19 × 0.16 × 0.16	0.2 × 0.18 × 0.03
Radiation	Cu Kα (λ = 1.54184)	Ga Kα (λ = 1.3405)	Cu Kα (λ = 1.54184)
2Θ range for data collection/°	9.846 to 152.974	8.804 to 121.342	4.974 to 153.492
Index ranges	$-6 \le h \le 7$, $-13 \le k \le 13$, $-19 \le l \le 19$	$-12 \le h \le 12$, $-8 \le k \le 7$, $-21 \le l \le 21$	$-7 \le h \le 8$, $-12 \le k \le 11$, $-44 \le l \le 44$
Reflections collected	11696	14841	14315
Independent reflections	2210 [R_{int} = 0.0255, R_{sigma} = 0.0146]	2560 [R_{int} = 0.0294, R_{sigma} = 0.0187]	4540 [R_{int} = 0.0222, R_{sigma} = 0.0218]
Data/restraints/parameters	2210/0/163	2560/0/163	4540/0/340
Goodness-of-fit on F^2	1.054	1.068	1.027
Final R indexes [I>=2σ (I)]	R_1 = 0.0325, wR_2 = 0.0817	R_1 = 0.0333, wR_2 = 0.0863	R_1 = 0.0284, wR_2 = 0.0748
Final R indexes [all data]	R_1 = 0.0326, wR_2 = 0.0818	R_1 = 0.0377, wR_2 = 0.0892	R_1 = 0.0308, wR_2 = 0.0762
Largest diff. peak/hole / e Å^{-3}	0.58/-0.42	0.28/-0.38	0.31/-0.23

Table S2. Crystal structure data and structural refinement for **MQ7-i**, **MQ7-o** and **MQ7-m**.

Compound	MQ7-i	MQ7-o	MQ7-m
CCDC Number	2131929	2131978	2131930
Empirical formula	$C_{230}H_{172}Cl_{12}N_{18}O_{12}S_9Se_3$	$C_{166}H_{144}Cl_8N_{12}O_8S_6Se_2$	$C_{131}H_{109}Cl_8N_{12}O_8S_6Se_2$
Formula weight	4330.67	3068.80	2613.18
Temperature/K	99.99(10)	100.00(10)	100.00(11)
Crystal system	triclinic	triclinic	triclinic
Space group	P-1	P-1	P-1
a/Å	13.5876(2)	12.7325(7)	14.1732(3)
b/Å	22.1745(3)	15.7208(8)	15.6986(3)
c/Å	26.3983(4)	22.6533(11)	22.3448(4)
α/°	70.7660(10)	88.007(4)	80.066(2)
β/°	85.9980(10)	79.532(4)	73.691(2)
γ/°	82.0080(10)	75.379(4)	74.133(2)
Volume/Å^3	7434.40(19)	4314.2(4)	4565.10(17)
Z	1	1	1
ρ_{calc}g/cm^3	0.967	1.181	0.951
μ/mm^{-1}	2.403	1.841	2.565
F(000)	2224.0	1588.0	1343.0
Crystal size/mm^3	0.15 × 0.1 × 0.05	0.03 × 0.02 × 0.01	0.14 × 0.12 × 0.09
Radiation	Cu Kα (λ = 1.54184)	Ga Kα (λ = 1.3405)	Cu Kα (λ = 1.54184)
2Θ range for data collection/°	4.252 to 154.252	5.052 to 122.492	4.142 to 154.272
Index ranges	-17 ≤ h ≤ 16, -27 ≤ k ≤ 27, -27 ≤ l ≤ 33	-16 ≤ h ≤ 16, -20 ≤ k ≤ 20, -20 ≤ l ≤ 29	-17 ≤ h ≤ 17, -19 ≤ k ≤ 19, -24 ≤ l ≤ 28
Reflections collected	112468	59046	56385
Independent reflections	29749 [R_{int} = 0.0531, R_{sigma} = 0.0422]	19338 [R_{int} = 0.0415, R_{sigma} = 0.0491]	18292 [R_{int} = 0.0679, R_{sigma} = 0.0466]
Data/restraints/parameters	29749/148/1291	19338/254/913	18292/7/773
Goodness-of-fit on F^2	1.123	1.452	1.732
Final R indexes [I>=2σ (I)]	R_1 = 0.0927, wR_2 = 0.2827	R_1 = 0.1231, wR_2 = 0.3692	R_1 = 0.1416, wR_2 = 0.3819
Final R indexes [all data]	R_1 = 0.1164, wR_2 = 0.3100	R_1 = 0.1711, wR_2 = 0.4071	R_1 = 0.1761, wR_2 = 0.4272
Largest diff. peak/hole / e Å^{-3}	1.05/-0.40	1.55/-0.78	2.22/-0.81

Table S3. Photovoltaic parameters of PSCs based on **PM6:MQ7-i** under the illumination of AM 1.5G (100 mW/cm^2).

CN (vol %)	Annealing temperature [^{o}C]	Annealing time [min]	V_{OC} [V]	J_{SC} [mA cm^{-2}]	FF [%]	PCE [%]
0.3	80	5	0.86	22.42	63.80	12.34
0.5	80	5	0.87	23.78	64.76	13.32
0.8	80	5	0.86	23.16	62.52	12.47
0.5	70	5	0.87	23.02	64.53	12.92
0.5	90	5	0.87	23.68	63.57	13.05
0.5	80	3	0.87	23.47	64.27	13.07
0.5	80	7	0.86	24.06	63.57	13.19

Table S4. Photovoltaic parameters of PSCs based on **PM6:MQ7-o** under the illumination of AM 1.5G (100 mW/cm^2).

CN (vol %)	Annealing temperature [^{o}C]	Annealing time [min]	V_{OC} [V]	J_{SC} [mA cm^{-2}]	FF [%]	PCE [%]
0.3	80	5	0.90	20.99	60.79	11.51
0.5	80	5	0.91	22.30	65.23	13.29
0.8	80	5	0.90	21.74	62.12	12.19
0.5	70	5	0.91	21.09	63.77	12.27
0.5	90	5	0.91	20.43	64.82	12.10
0.5	80	3	0.91	21.89	60.74	12.12
0.5	80	7	0.91	21.33	64.27	12.50

Table S5. Photovoltaic parameters of PSCs based on **PM6:MQ7-m** under the illumination of AM 1.5G (100 mW/cm^2).

CN (vol %)	Annealing temperature [^{o}C]	Annealing time [min]	V_{OC} [V]	J_{SC} [mA cm^{-2}]	FF [%]	PCE [%]
0.3	80	5	0.86	22.29	60.07	11.55
0.5	80	5	0.86	23.44	60.56	12.27
0.8	80	5	0.86	22.51	60.35	11.75
0.5	70	5	0.86	23.52	59.52	12.11
0.5	90	5	0.86	23.54	59.87	12.19
0.5	80	3	0.87	22.38	60.42	11.96
0.5	80	7	0.86	22.95	60.72	12.06

Table S6. Summarized parameters of the ordered structure from GIWAXS.

Sample	π-π stacking		Lamellar stacking	
	d-spacing (Å）	CL (Å)	d-spacing (Å）	CL (Å)
MQ7-i	3.49	19.38	19.06	73.27
MQ7-o	3.54	20.93	19.16	72.67
MQ7-m	3.50	20.95	19.10	87.66
PM6:MQ7-i	3.58	18.93	19.87	90.86
PM6:MQ7-o	3.61	19.93	20.33	78.74
PM6:MQ7-m	3.59	20.44	19.97	82.61

9. Supplementary figures

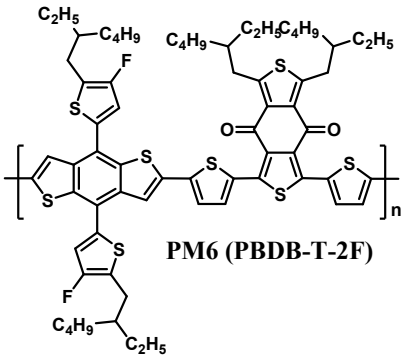

Figure S1. Molecular structure of donor PM6 (PBDB-T-2F).

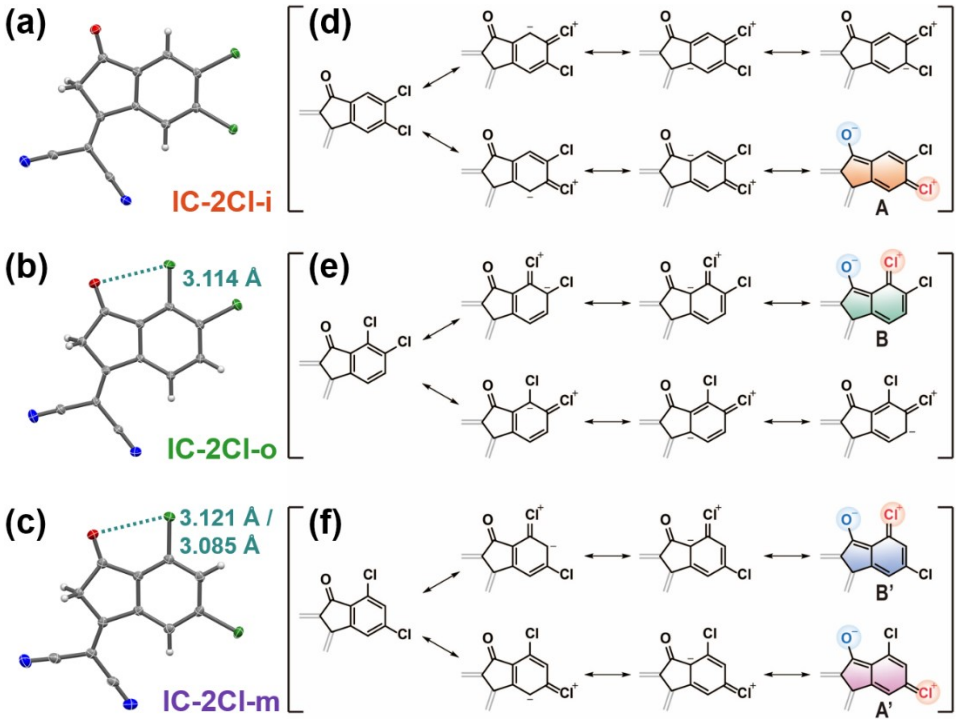

Figure S2. Single-crystal structures of three end groups (a-c), and the resonance analysis about the oxygen atoms, the chlorine atoms and the arene rings of relative end groups (d-f).

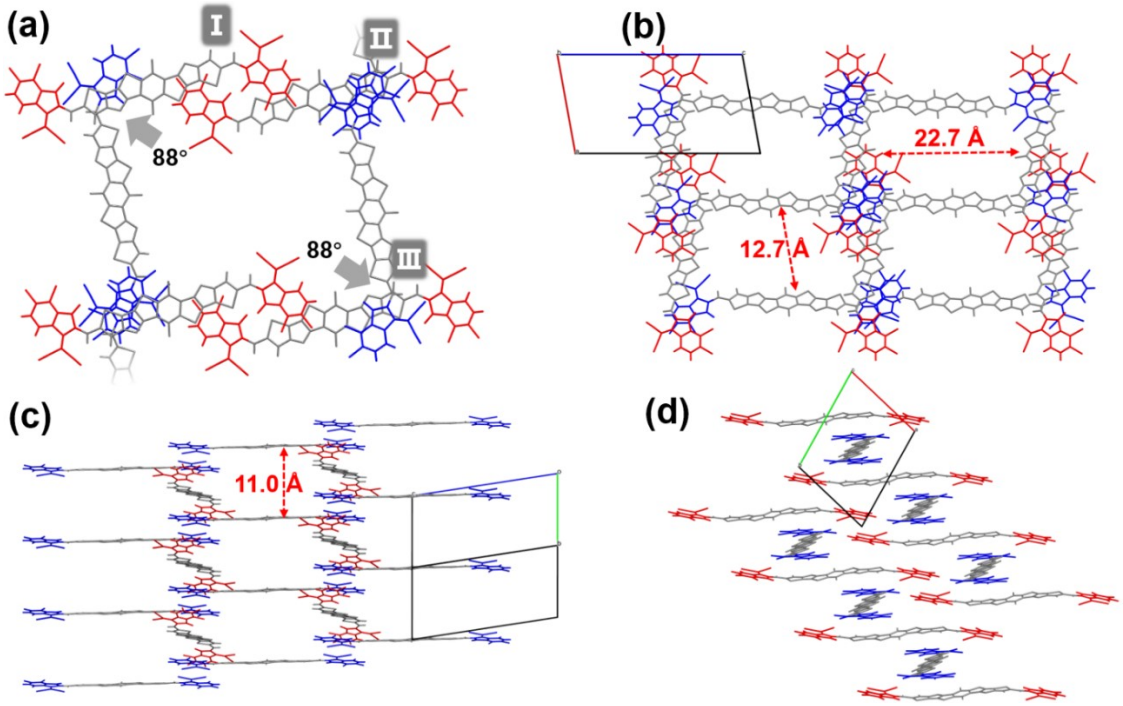

Figure S3. (a) Molecular packing patterns and relative rotational angles of **MQ7-o**, the 3D network packing patterns of **MQ7-o** (b-d).

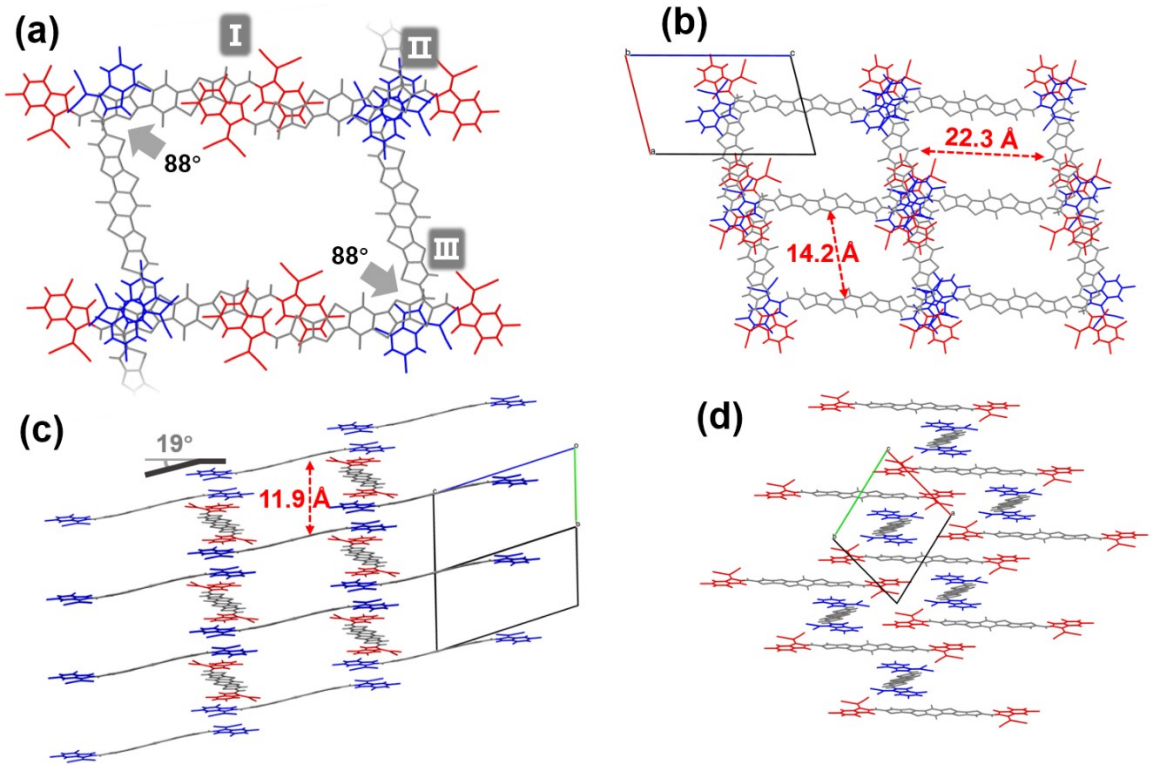

Figure S4. (a) Molecular packing patterns and relative rotational angles of **MQ7-m**, the 3D network packing patterns of **MQ7-m** (b-d).

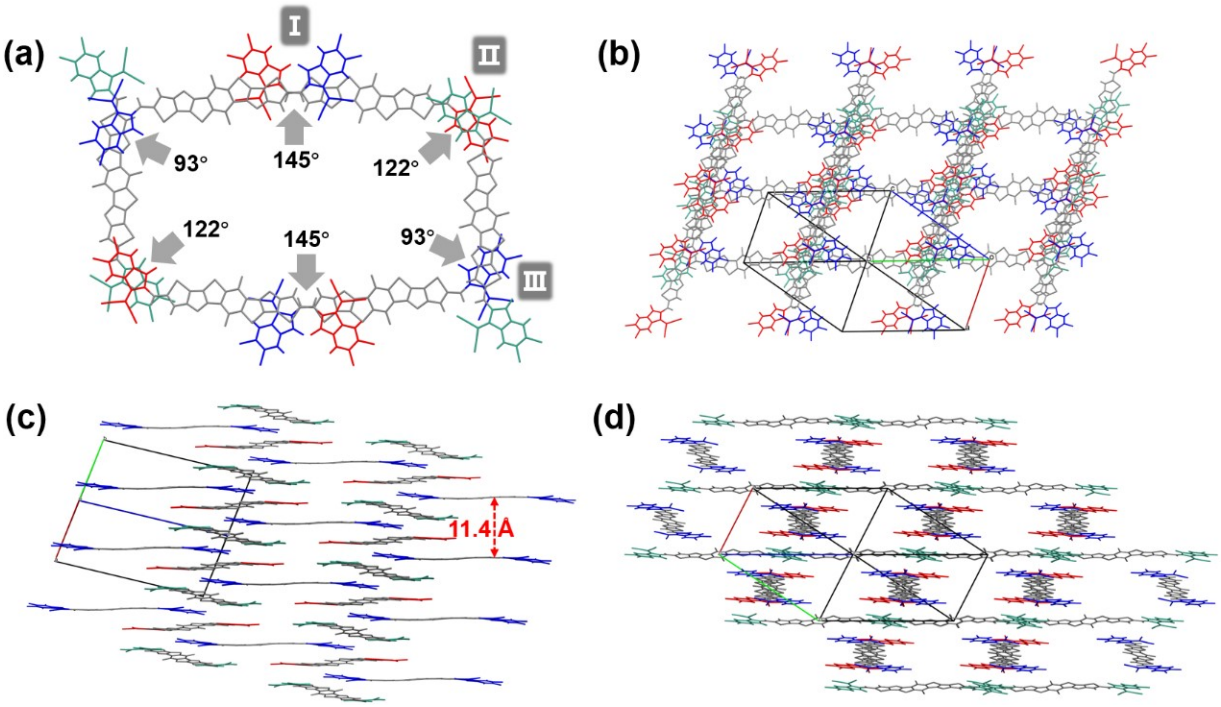

Figure S5. (a) Molecular packing patterns and relative rotational angles of **MQ7-i**, the 3D network packing patterns of **MQ7-i** (b-d).

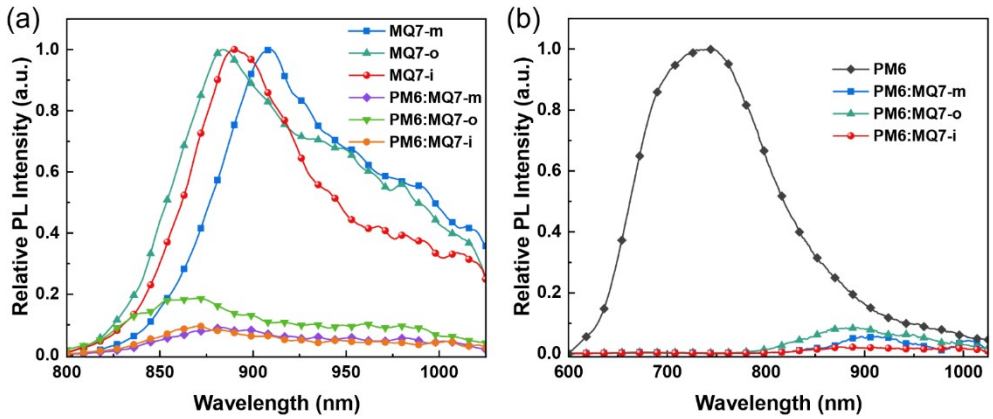

Figure S6. PL spectra of the pristine films as well as the correlative blend films: (a) excited at 780 nm; (b) excited at 550 nm.

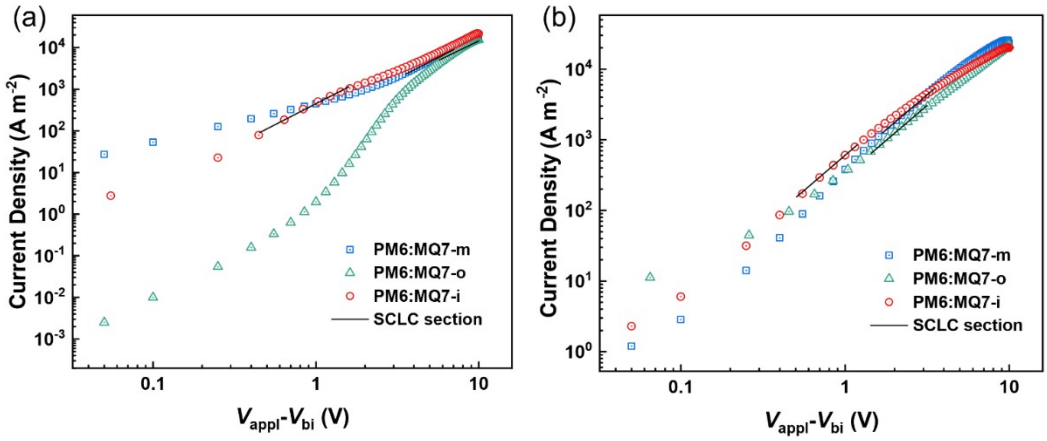

Figure S7. *J-V* curves of electron-only (a) and hole-only (b) devices based on **PM6:MQ7-i**, **PM6:MQ7-o**, and **PM6:MQ7-m**.

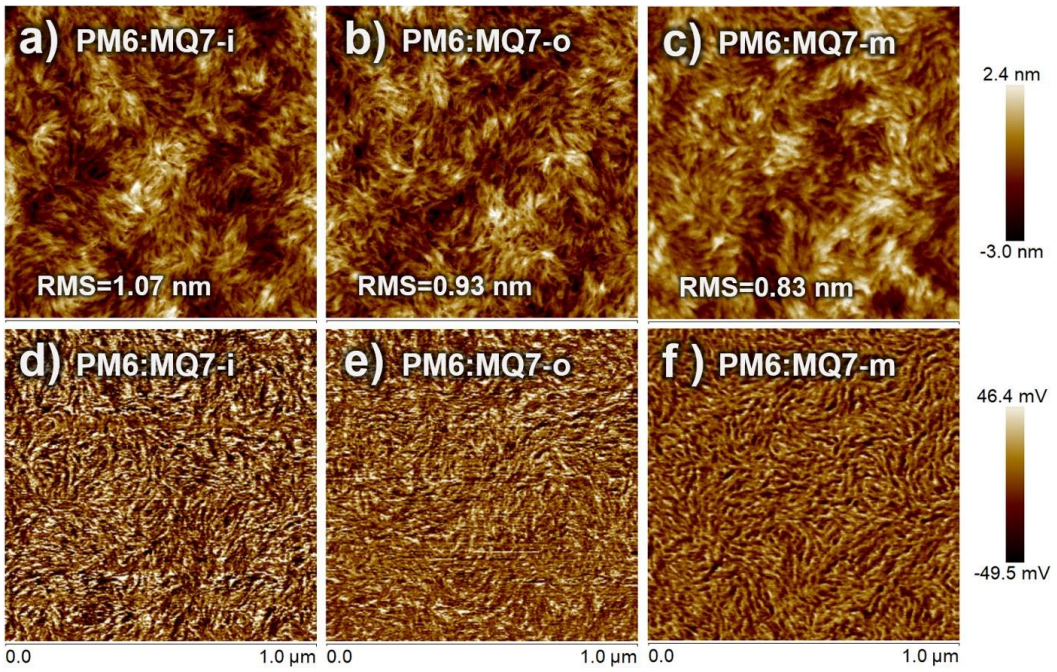

Figure S8. AFM height images of blend films based on **PM6:MQ7-i** (a), **PM6:MQ7-o** (b) and **PM6:MQ7-m** (c), and AFM adhesion images of blend films based on **PM6:MQ7-i** (d), **PM6:MQ7-o** (e) and **PM6:MQ7-m** (f).

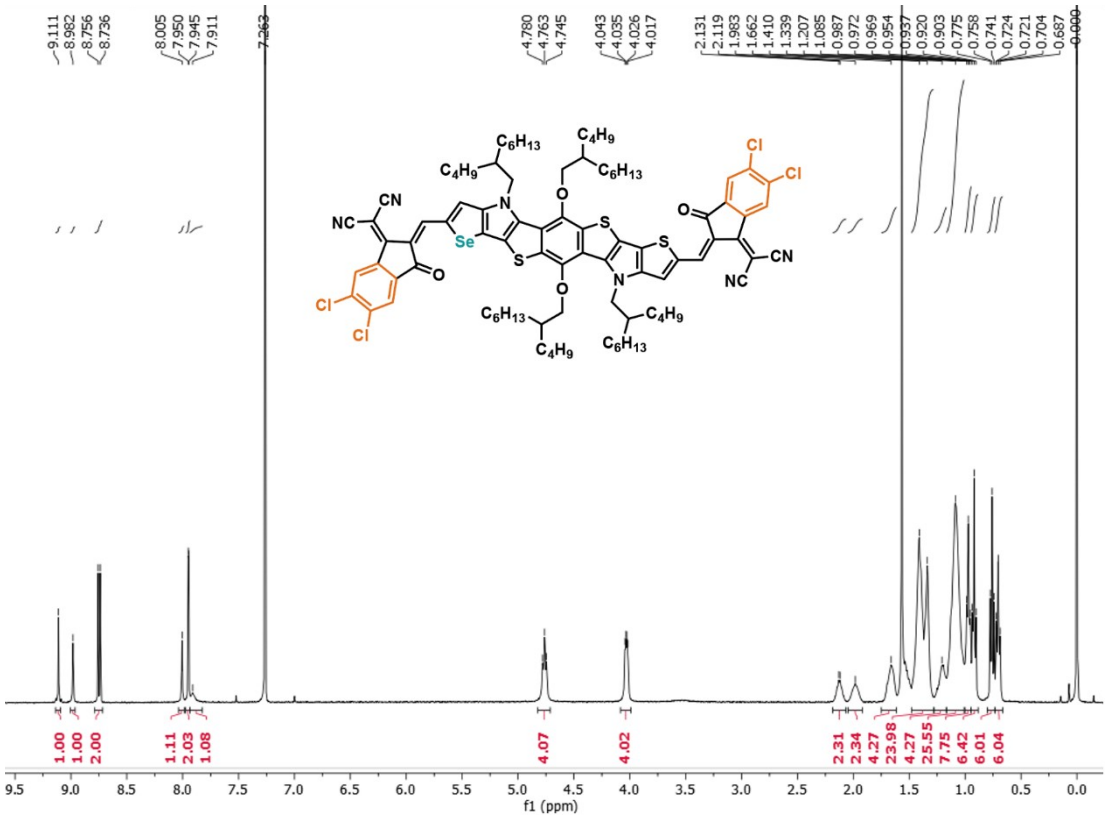

Figure S9. ^{1}H NMR spectrum for **MQ7-i**.

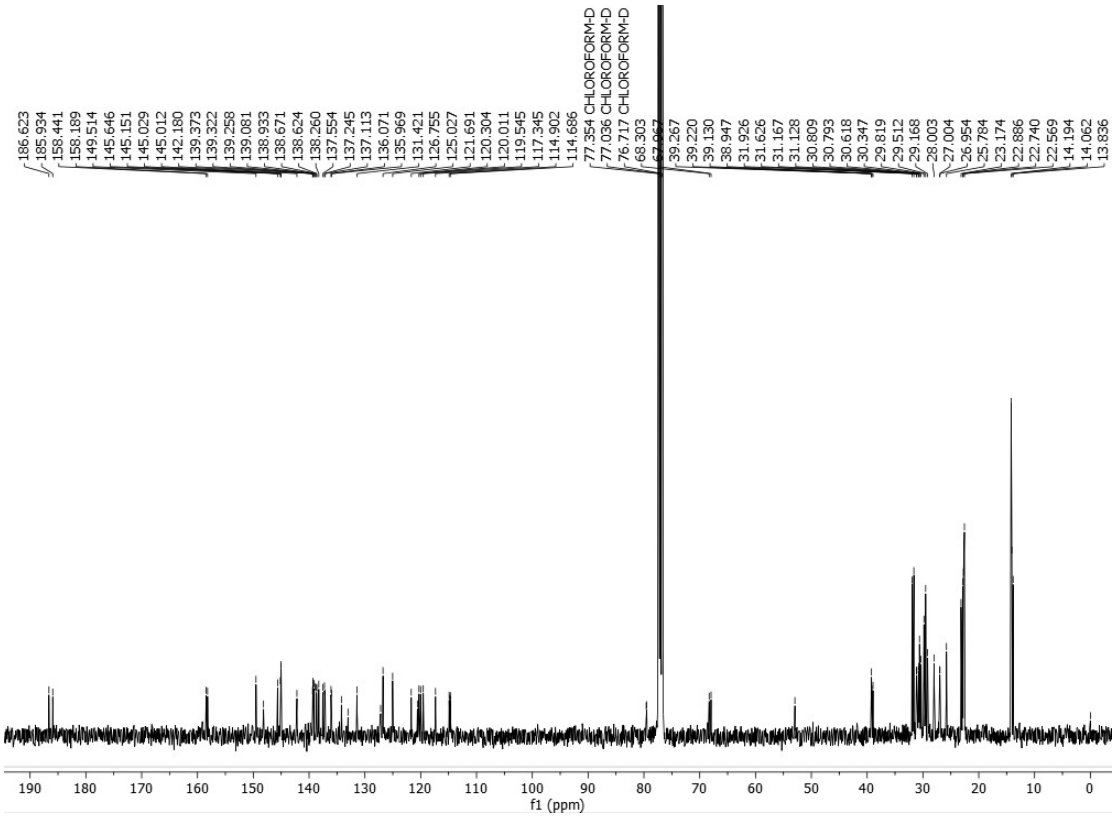

Figure S10. ^{13}C NMR spectrum for **MQ7-i**.

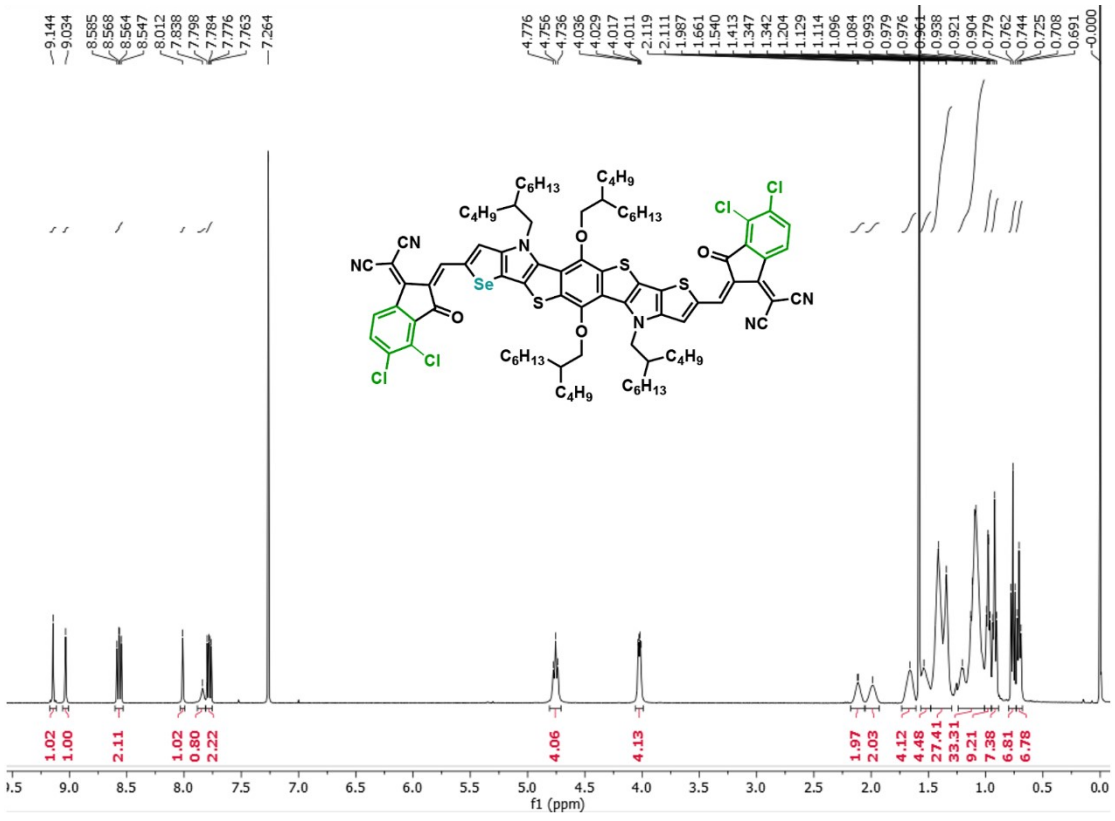

Figure S11. ^{1}H NMR spectrum for **MQ7-o**.

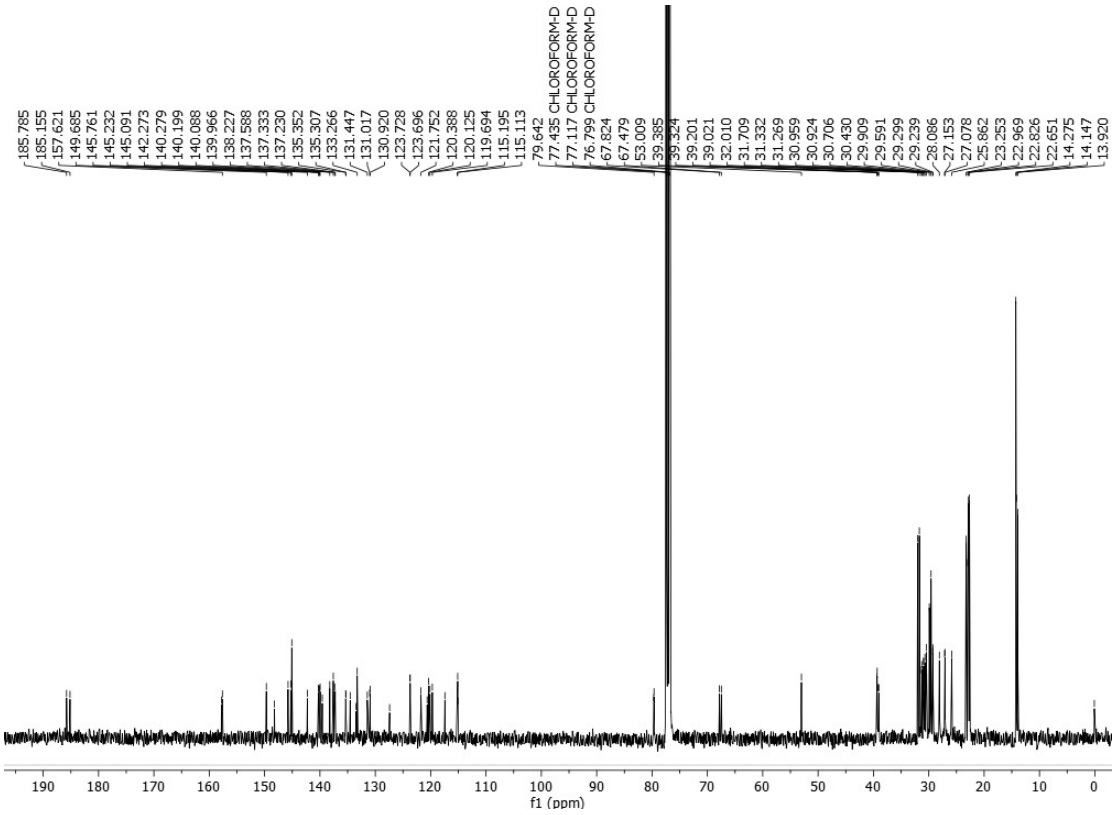

Figure S12. ^{13}C NMR spectrum for **MQ7-o**.

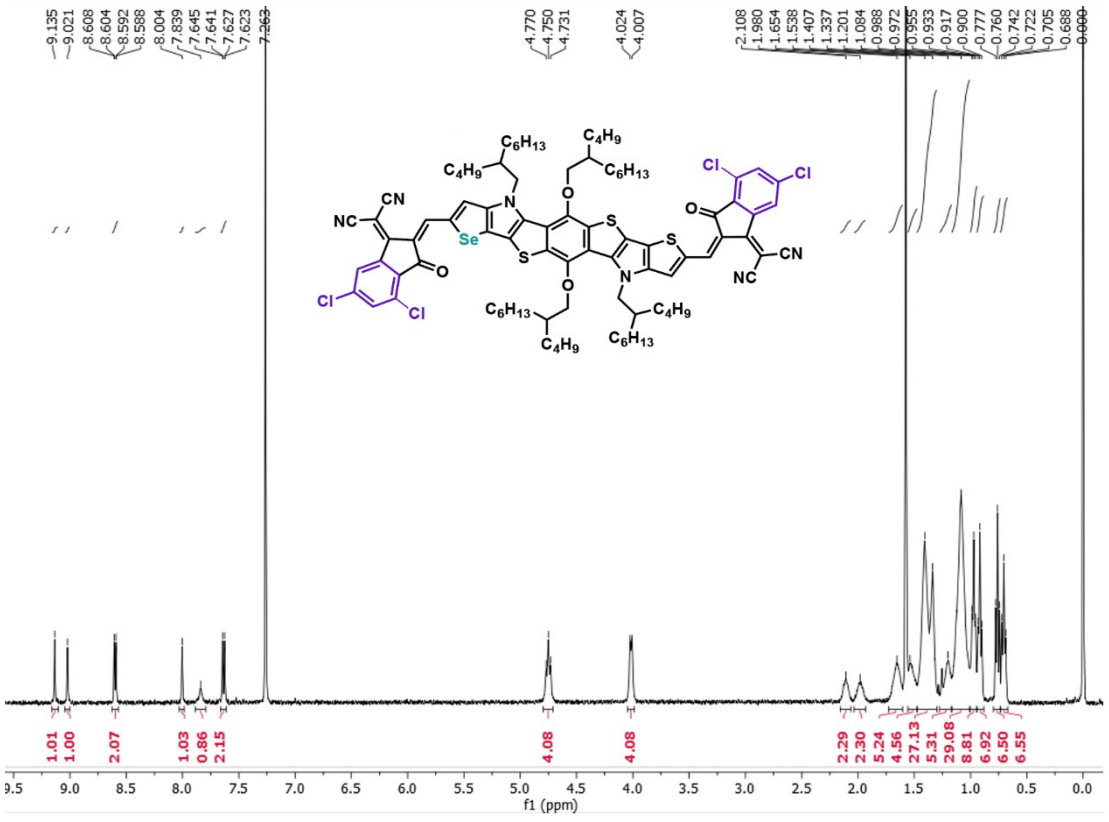

Figure S13. ^{1}H NMR spectrum for **MQ7-m**.

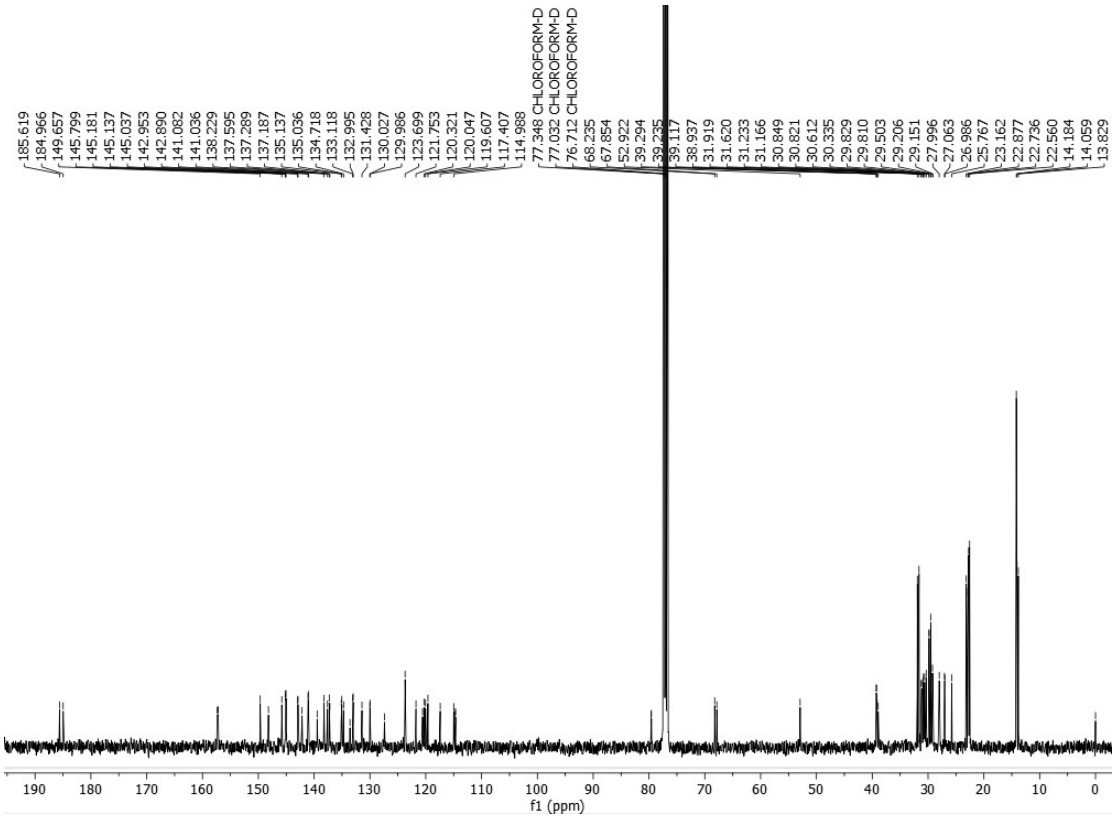

Figure S14. ^{13}C NMR spectrum for **MQ7-m**.

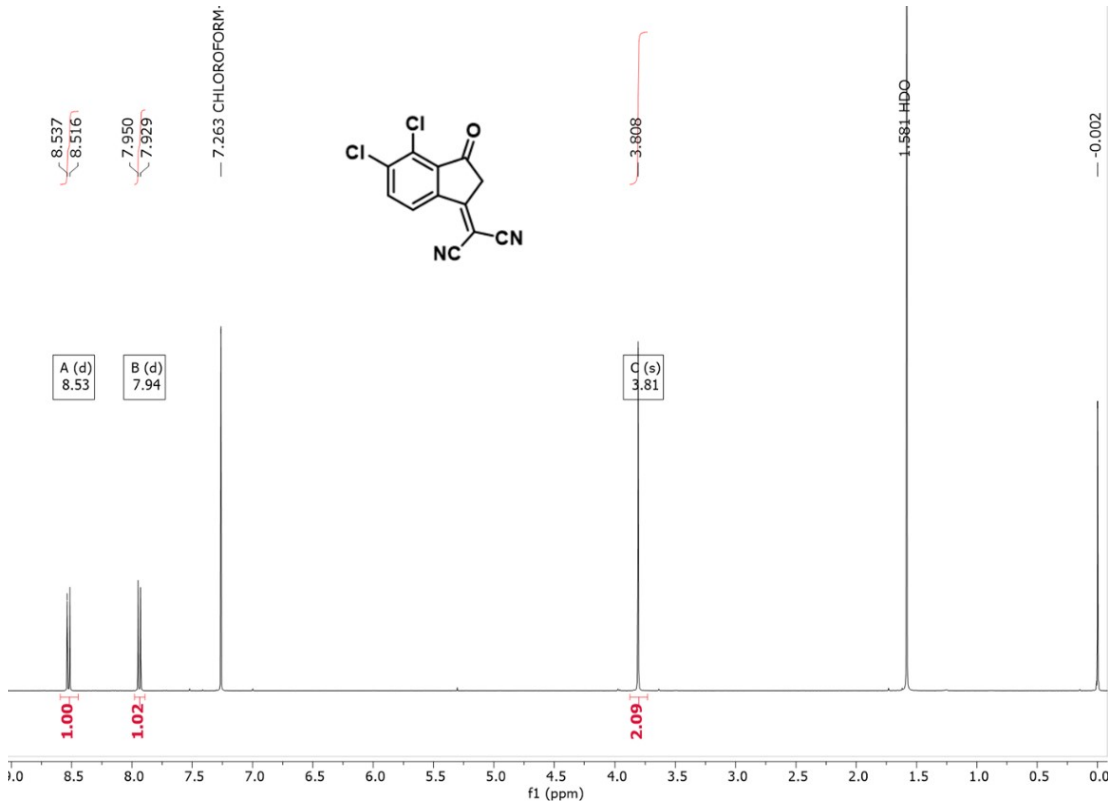

Figure S15. ^{1}H NMR spectrum for **IC-2Cl-o**.

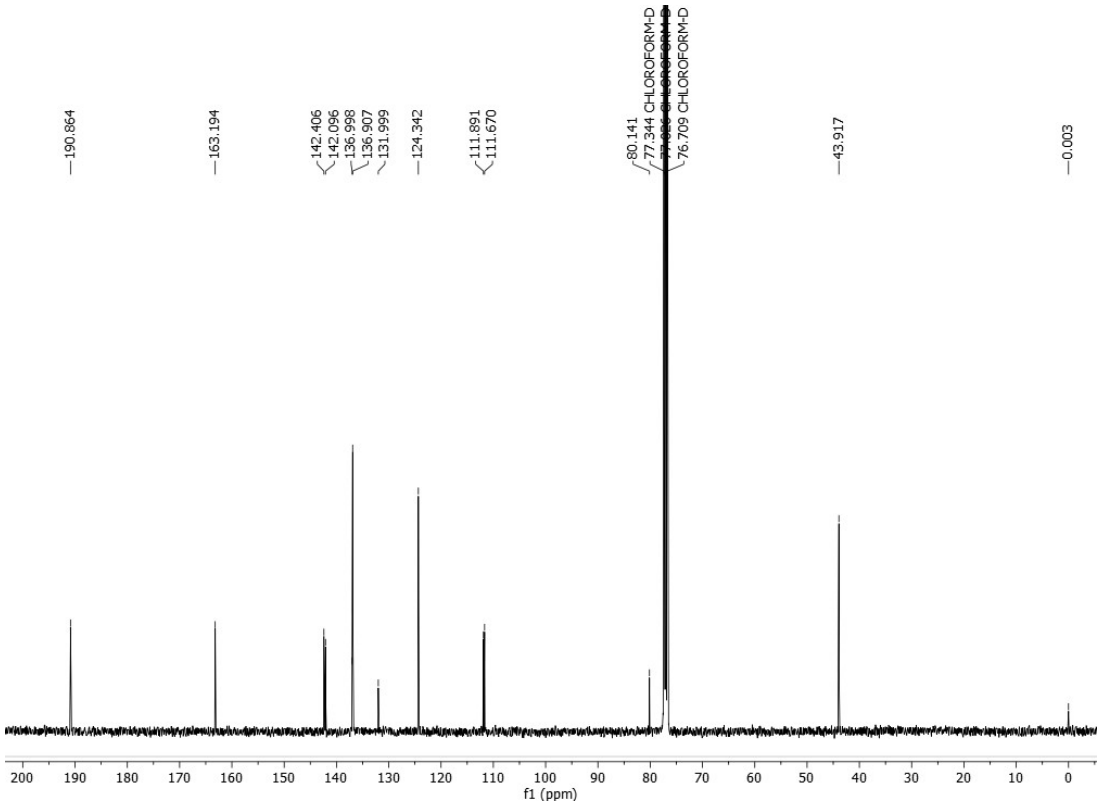

Figure S16. ^{13}C NMR spectrum for **IC-2Cl-o**.

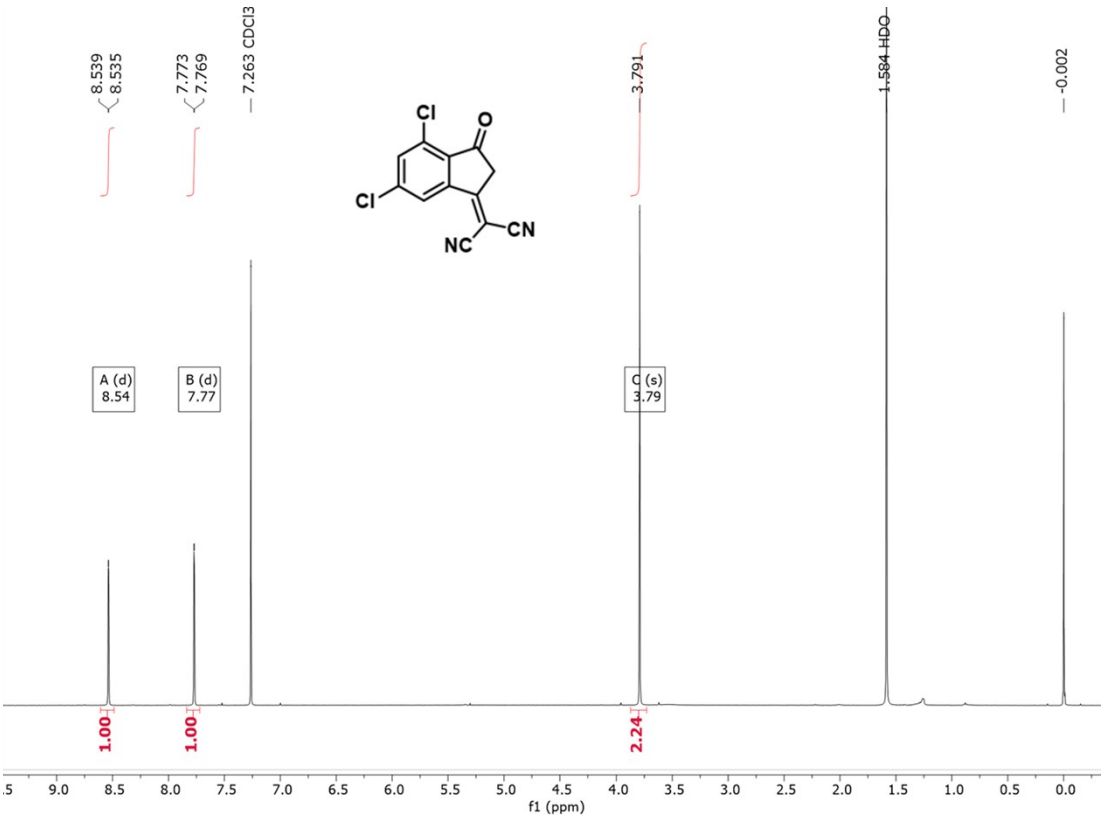

Figure S17. ^{1}H NMR spectrum for **IC-2Cl-m**.

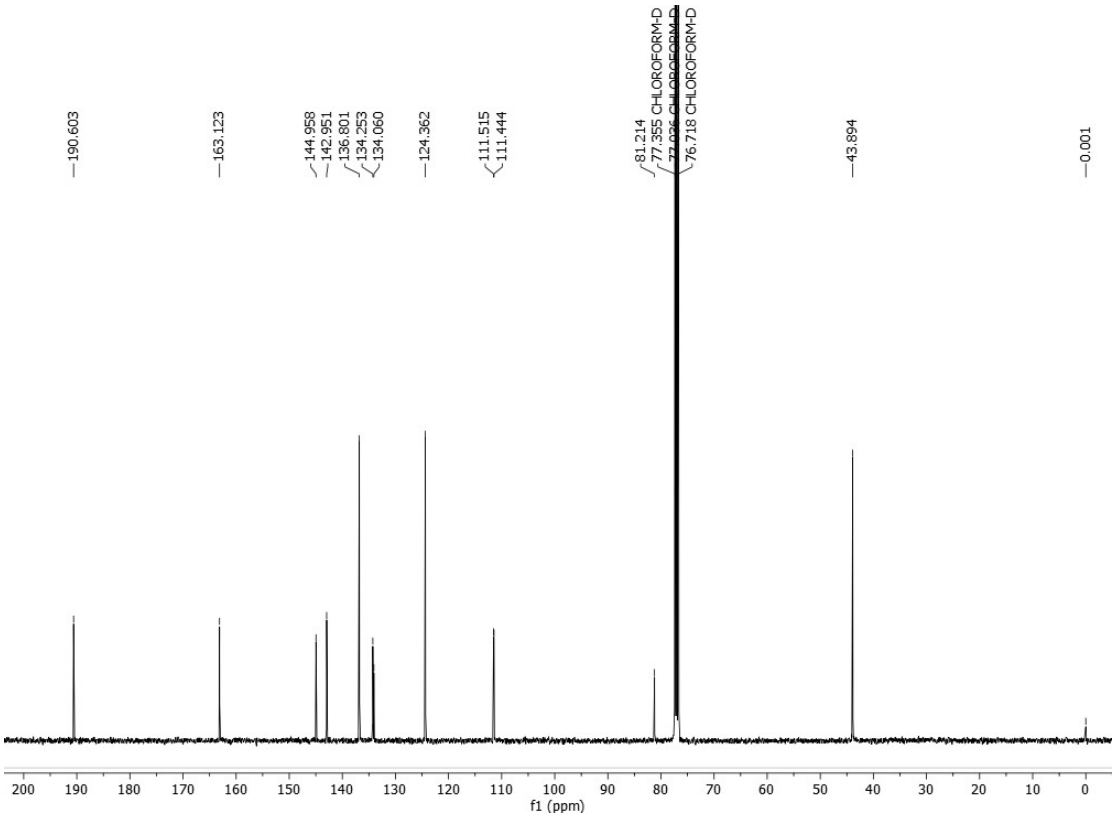

Figure S18. ^{13}C NMR spectrum for **IC-2Cl-m**.

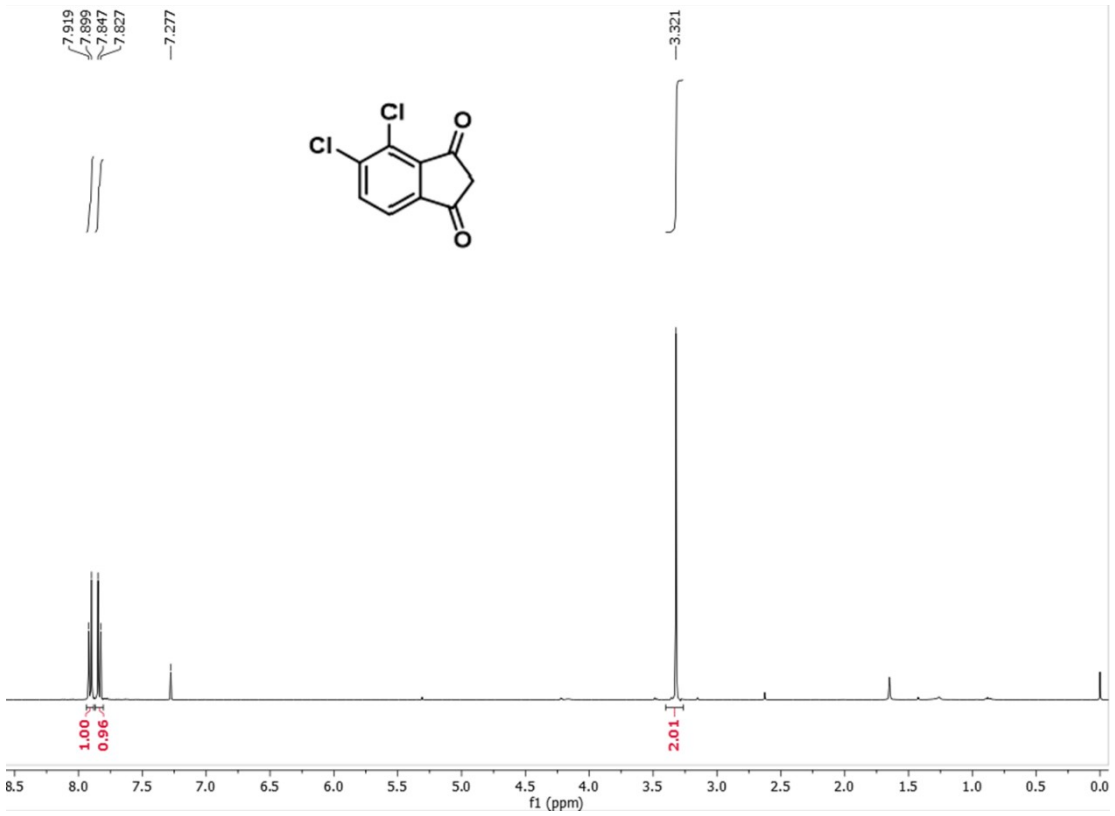

Figure S19. ^{1}H NMR spectrum for compound **3**.

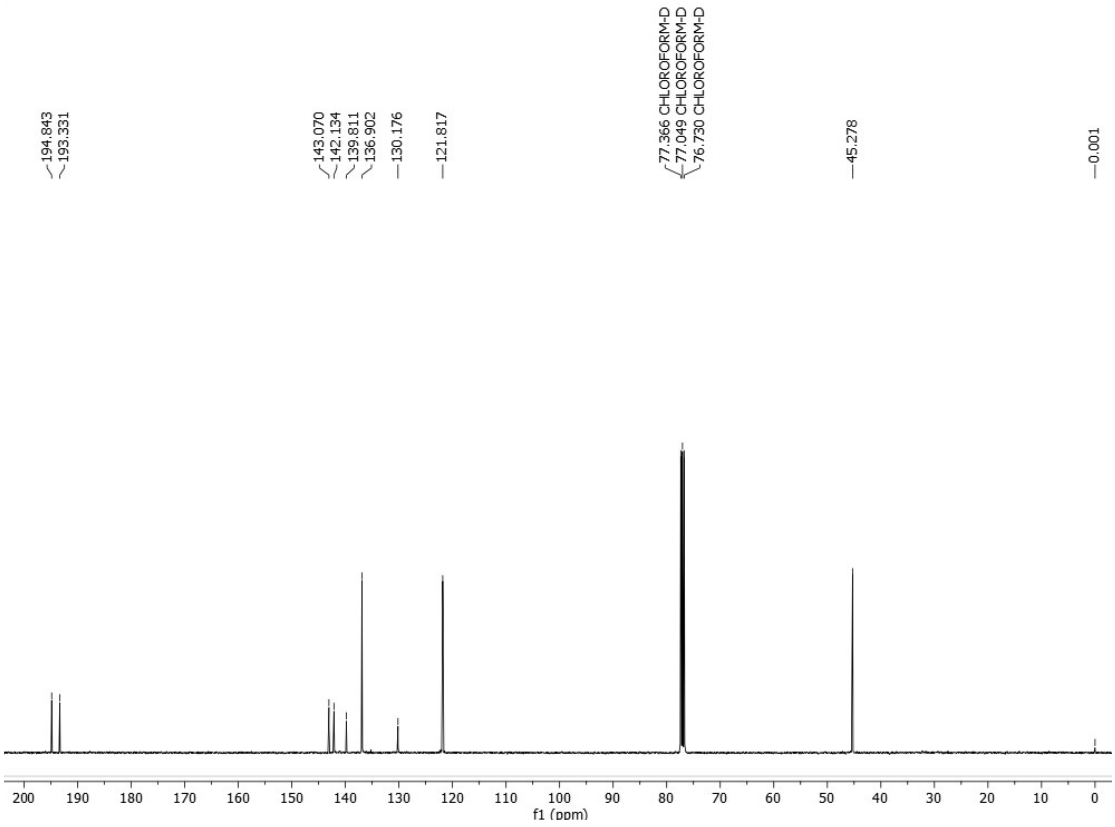

Figure S20. ^{13}C NMR spectrum for compound **3**.

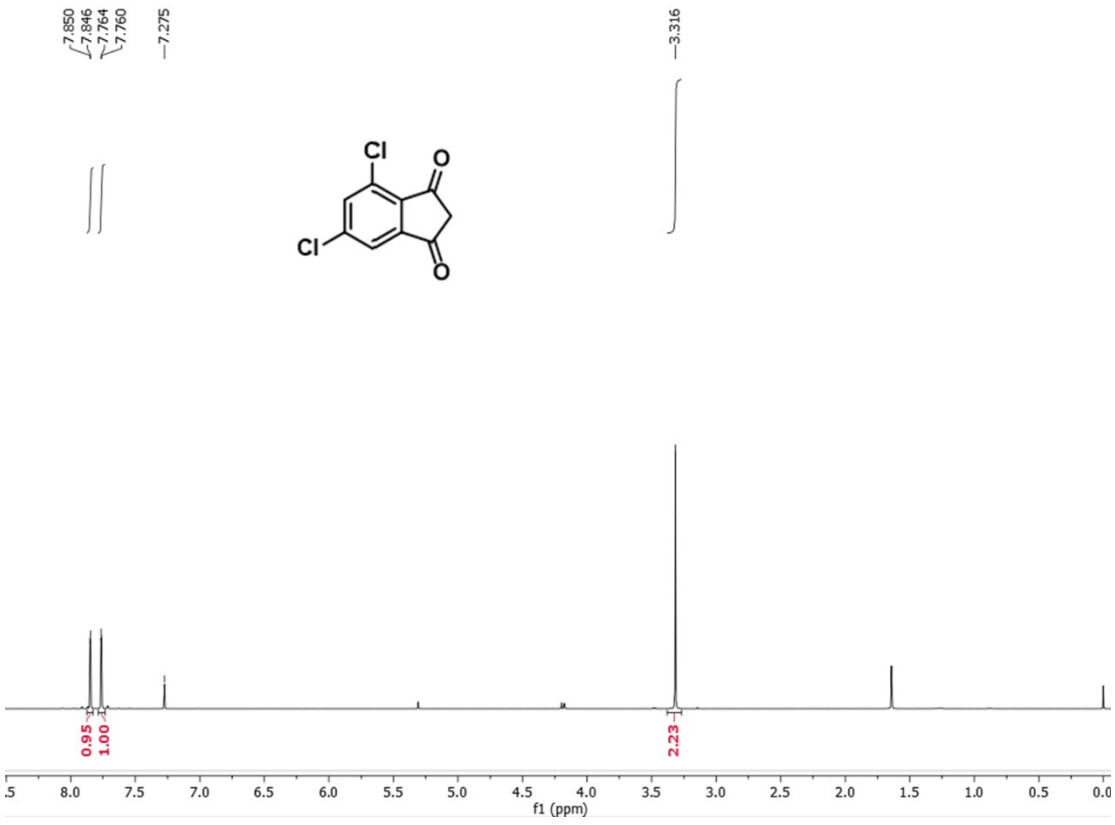

Figure S21. ^{1}H NMR spectrum for compound **5**

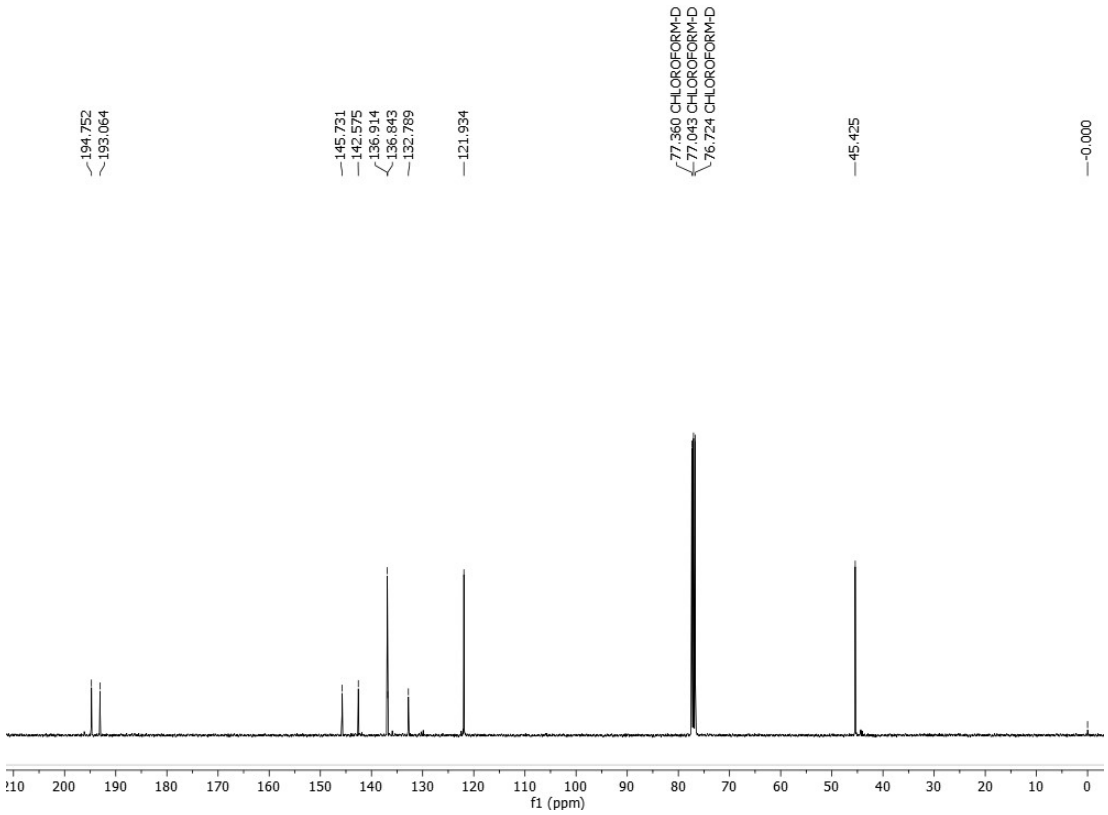

Figure S22. ^{13}C NMR spectrum for compound **5**.

References

[1] G. Sartori, F. Bigi, R. Maggi, D. Baraldi, G. Casnati, *J. Chem. Soc., Perkin trans.* 1, **1992**, 2985-2988.